RESEARCH PAPER

A Variable Parameter Linear Tracking Differentiator and Its Application in Large Ground-based Telescopes

Research in Astronomy and Astrophysics, 22:125013 (11pp), 2022 December https://doi.org/10.1088/1674-4527/ac9aee

A Variable Parameter Linear Tracking Differentiator and Its Application in Large Ground-based Telescopes

Xiao-Xia Yang, Yong-Ting Deng, Jian-Li Wang, and Bin Zhang
Changchun Institute of Optics, Fine Mechanics and Physics, Chinese Academy of Sciences, Changchun 130033, China; yxxair@163.com, dyt0612@163.com
Received 2022 July 8; revised 2022 September 6; accepted 2022 September 27; published 2022 December 7

Abstract

This paper is concerned with the characteristics of a tracking differentiator (TD) in arranging transition process for the physical system. In order to overcome disadvantages of linear TD (LTD) in practice, a novel variable parameter linear tracking differentiator (VLTD) is proposed. By designing the speediness factor as a function of the tracking error, the VLTD can track a large range of set values with reasonable speed and acceleration. Analysis shows that VLTD can converge to its set value under certain conditions. Meanwhile, the speed and acceleration bounds are added to the VLTD, which guarantees that the proposed transition signal really plays a transitional role. The numerical simulation results emphasize necessity for adding speed and acceleration bounds to the VLTD. By comparing VLTD with the nonlinear TD (NLTD) in the simulations and experiments, VLTD can achieve almost the same performance as the NLTD while it is easier to be implemented.

Key words: methods: data analysis – methods: analytical – methods: numerical – telescopes

1. Introduction

A tracking differentiator (TD) is an important component of active disturbance rejection control (ADRC) (Han 2009) that was first proposed by Han (Han & Wang 1994; Han 1989). It has two main functions: one is to extract differential signals from signals which are not differentiable, and the other is to arrange the transition process for the physical signals. Previous studies related with TD are mainly focus on the properties of its first function, such as conditions for convergence (Qi et al. 2004; Wu et al. 2004; Guo & Zhao 2013; Zhang et al. 2021), filtering properties (Xie et al. 2019; Zhang et al. 2019; Yu & Jin 2021), differential signal extraction (Tang et al. 2009; Bu et al. 2015; Zhao et al. 2015; Yang et al. 2020) and tracking rapidity analysis (Tian et al. 2014).

As for TD's second function, it plays an important role in dealing with contradiction between the rapidity and overshoot of control systems and it has been widely used to solve engineering problems. However, there are rarely theoretical studies about TD as a tool for transition process arrangement. Han had analyzed the transitional time, maximum speed and acceleration of TD (Han 2009), but the analysis mainly considered the unit step response. The original intention for arranging the transition process is to construct a bridge between the reference signal and the feedback signal of the control system, which can guarantee that the control error will not grow sharply when the reference signal changes drastically. As the feedback capability of the physical system is always restricted by objective conditions (such as driving power supply, mechanical structure, driving force), so the proposed transition signal must match the feedback capability of the control system, otherwise it will not work as a transition bridge. Therefore, when we arrange the transition process in the engineering practice, the maximum speed and acceleration of the transition signal should be designed accordance with the feedback ability of the physical system. Generally, we denote the physical feedback signal of the control system as the position signal, and denote the first and second derivative of the physical signal as speed and acceleration signal respectively. In Section 2, by analyzing the commonly used TD methods, we can find how the TD parameters affect the speed and acceleration outputs of the transition process. Let $V_{\max}$ and $a_{\max}$ denote the upper bounds of the speed and acceleration of the physical system, respectively. Analysis shows that the maximum speed and acceleration of the transition process proposed by linear TD (LTD) have no constant upper bounds since they are both related to the set value p_0 (See Section 2.1). Meanwhile, it is infeasible by simply adding speed and acceleration upper bounds to LTD, because it will cause fluctuations in the position signal (See Section 2.1). Thus LTD with a constant parameter may not satisfy the requirement of arranging the transition process in the engineering practice. Although the nonlinear TD (NLTD) can give a transition process with constant acceleration upper bound, it has no constant speed upper bound and its calculation is somewhat complicated.

Above all, it is of great importance to propose a more practical tool for arranging the transition process for physical signals with speed and acceleration restrictions. In this paper, we will propose an improved variable parameter linear tracking

differentiator (VLTD) which overcomes the shortcomings of the commonly used methods and gives a more practical transition process. The remainder of the paper is organized as follows. Section 2 gives the analysis of the commonly used TD and Section 3 proposes the new VLTD. Sections 4 and 5 present the numerical simulation and experimental results with the proposed method. The main conclusions are delivered in Section 6.

2. Analysis of the Commonly Used TD

Although researchers have proposed various modified structures of TD, most of the studies mainly focus on the differential signal extraction performance. The commonly used tools for arranging transition processes are still LTD and NLTD proposed by Han (Han & Wang 1994; Han & Yuan 1999). In this section, we will give analysis of the performance of LTD and NLTD on arranging transition process.

2.1. LTD

The discrete form of LTD is as follows

$$\begin{cases} x_1(k+1) = x_1(k) + hx_2(k) \\ x_2(k+1) = x_2(k) + h(-r^2(x_1(k) - p_0(k)) - 2rx_2(k)) \end{cases} \tag{1}$$

where p_0 denotes the set value of the system, x_1 and x_2 are the outputs of LTD; h is the sampling time for the discrete system; r is the only parameter to be adjusted, which determines the properties of LTD. Assume that p_0 is a constant, and define the transition time T_0 as the time point when the state x_1 reaches $0.99p_0$ for the first time. Define V_{maxLTD} and a_{maxLTD} as the maximum absolute values of x_2 and $\dot{x}_2$, respectively. Table 1 shows the calculation results of the three indices T_0, V_{maxLTD} and a_{maxLTD} when the set value p_0 and parameter r change.

Using the curve fitting toolbox of MATLAB, we can obtain the fitting functions as follows

$$T_0 = \frac{6.671}{r^{1.004}},\ V_{\text{maxLTD}} = 0.3353p_0r^{1.031},\ a_{\text{maxLTD}} = p_0r^2 \tag{2}$$

Figure 1 shows the fitting curves of the three functions in (2) when $p_0 = 1$. The fitting result shows that T_0 is almost inversely proportional to the parameter r, but independent of the final value p_0. Meanwhile, both V_{maxLTD} and a_{maxLTD} are closely related to p_0. If V_{maxLTD} and a_{maxLTD} are far greater than the maximum speed and acceleration of the physical system, the feedback signal will not track the transition signal. Thus, LTD will not serve the purpose of arranging the transition process. We can deduce that it will cause position fluctuations by simply adding speed and acceleration upper bounds to LTD. Let $p_0 = 100$, $r = 15$, $h = 0.001$, then according to Equation (2), we can calculate the maximum speed and acceleration of the transition signal as follows

$$V_{\text{maxLTD}} = 547,\ a_{\text{maxLTD}} = 22500$$

Assume that the upper bounds of speed and acceleration of the feedback signals are as follows

$$V_{\max} = 21,\ a_{\max} = 12 \tag{3}$$

Figure 2 shows the output signals of LTD when we simply set $V_{\max}$ and $a_{\max}$ as the speed and acceleration upper bounds.

Table 1
The Calculation Results of the LTD

r	$p_0 = 1$			$p_0 = 10$		
	T_0	V_{maxLTD}	a_{maxLTD}	T_0	V_{maxLTD}	a_{maxLTD}
5	1.326	1.844	25	1.326	18.440	250
10	0.663	3.697	100	0.663	36.973	1000
15	0.441	5.560	225	0.441	55.601	2250
20	0.331	7.432	400	0.331	74.320	4000
25	0.264	9.314	625	0.264	93.137	6250
30	0.220	11.206	900	0.220	112.060	9000
35	0.188	13.108	1225	0.188	131.079	12250
40	0.165	15.017	1600	0.165	150.165	16000
45	0.146	16.940	2025	0.146	169.402	20250
50	0.131	18.868	2500	0.131	88.677	25000
55	0.119	20.813	3025	0.119	208.132	30250
60	0.109	22.796	3600	0.109	227.688	36000
65	0.101	24.733	4225	0.101	247.332	42250
70	0.093	26.706	4900	0.093	267.056	49000
75	0.087	28.692	5625	0.087	286.924	56250
80	0.082	30.692	6400	0.082	306.922	64000
85	0.077	32.692	7225	0.077	326.920	72250
90	0.072	34.697	8100	0.072	346.970	81000
95	0.069	36.752	9025	0.069	67.523	90250
100	0.065	38.742	10000	0.065	387.420	100000

2.2. NLTD

Han had derived the fastest discrete TD by adopting the function fhan, which converges in limited steps with the acceleration restriction r. The NLTD using fhan is designed as follows

$$\begin{cases} x_1(k+1) = x_1(k) + hx_2(k) \\ x_2(k+1) = x_2(k) + h\text{fhan}(x_1(k) - p_0(k), x_2(k), r, h_0) \end{cases} \tag{4}$$

where fhan is the following nonlinear function

$$\begin{cases} d = rh^2 \\ a_0 = hx_2 \\ y = x_1 + a_0 \\ a_1 = d(d + 8|y|) \\ a_2 = a_0 + \text{sgn}(y)(a_1 - d)/2 \\ a = (a_0 + y)\text{fsg}(y, d) + a_2(1 - \text{fsg}(y, d)) \\ \text{fhan} = -r(a/d)\text{fsg}(a, d) - r\,\text{sgn}(a)(1 - \text{fsg}(a, d)) \end{cases} \tag{5}$$

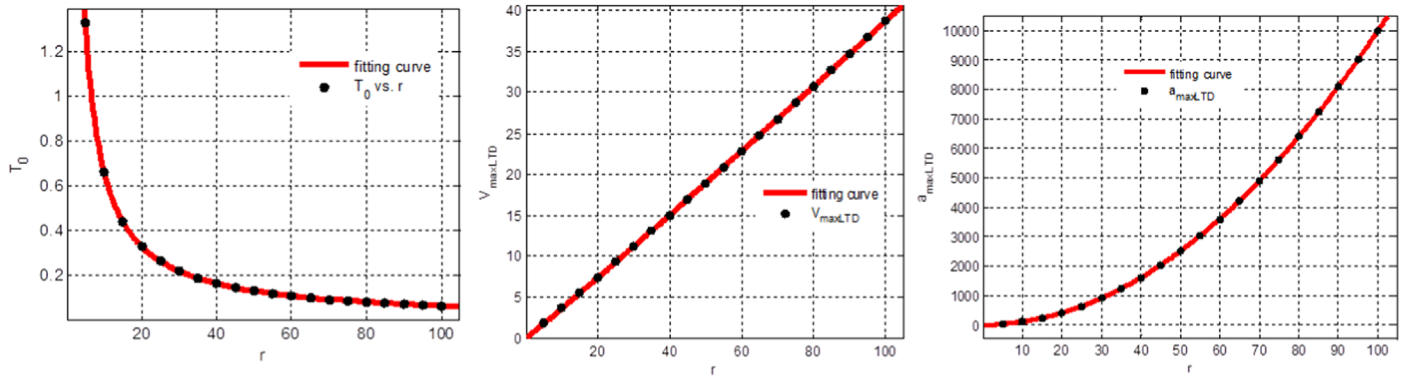

Figure 1. Fitting curves of the relationship between r and T_0, V_{maxLTD}, a_{maxLTD}.

where $\text{fsg}(a, d) = (\text{sgn}(x + d) - \text{sgn}(x - d))/2$.

The relationships between r, p_0 and T_0, V_{maxNLTD}, a_{maxNLTD} are as follows

$$T_0 = 2\sqrt{\frac{p_0}{r}},\ V_{\text{maxLTD}} = \sqrt{p_0 r},\ a_{\text{maxLTD}} = r \tag{6}$$

It can be seen that the acceleration has the upper bound r, but the maximum value of the speed has no upper bound since it is closely related to p_0. Actually, it is feasible to simply add speed upper bound to NLTD as follows

$$\begin{cases} x_2(k) = \text{sgn}(x_2(k))\min(|x_2(k)|, V_{\max}) \\ x_1(k+1) = x_1(k) + hx_2(k) \\ x_2(k+1) = x_2(k) + h\text{fhan}(x_1(k) - p_0(k), x_2(k), r, h_0) \end{cases} \tag{7}$$

Figure 3 gives the output signals of NLTD with speed upper bound $V_{\max}$. The parameters are the same as (3) and $h = 0.001$, $h_0 = 0.01$.

NLTD with speed upper bound gives an excellent transition process for the physical system which can maximize the tracking ability of the system. But we can see that the implementation of the function fhan is somewhat complicated in the engineering practice. In this paper, we will propose a new variable parameter LTD (VLTD) whose parameter r is the function of the tracking error, which can effectively overcome the shortcomings of the LTD and is implemented more easily than NLTD.

3. The Variable Parameter Linear Tracking Differentiator

The continuous form of VLTD is as follows

$$\begin{cases} \dot{x}_1(t) = x_2(t) \\ \dot{x}_2(t) = -r_1(t)^2(x_1(t) - p_0(t)) - 2r_1(t)x_2(t) \end{cases} \tag{8}$$

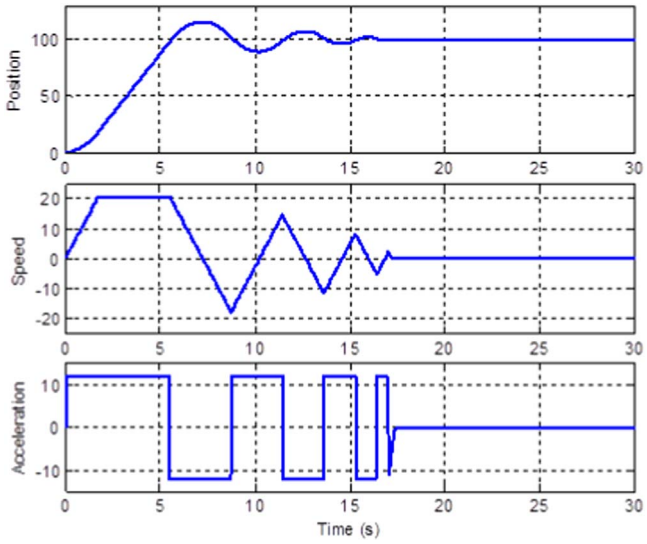

Figure 2. The outputs of the LTD with speed and acceleration upper bounds.

where the time-varying parameter $r_1(t)$ is designed as follows

$$r_1(t) = \begin{cases} \dfrac{\sigma\sqrt{r}}{\sqrt{|x_1(t) - p_0(t)|}} & if|x_1(t) - p_0(t)| \geqslant 1 \\ \sigma\sqrt{r} & if|x_1(t) - p_0(t)| < 1 \end{cases} \tag{9}$$

where r can be chosen as the maximum acceleration of the physical system, $\sigma \geqslant 1$ is the only parameter to be tuned.

$$\begin{cases} \dot{x}_1(t) = x_2(t) \\ \dot{x}_2(t) = \begin{cases} -\sigma^2 r\,\text{sgn}(x_1(t) - p_0(t)) - 2\sigma\sqrt{r}x_2(t)/\sqrt{|x_1(t) - p_0(t)|} & if|x_1(t) - p_0(t)| \geqslant 1 \\ -\sigma^2 r(x_1(t) - p_0(t)) - 2\sigma\sqrt{r}x_2(t) & if|x_1(t) - p_0(t)| < 1 \end{cases} \end{cases} \tag{10}$$

The difference between VLTD and LTD is that when the tracking error is larger than 1, parameter r_1 will be a time-varying parameter. When the tracking error is less than 1, then VLTD becomes LTD. The convergence properties of VLTD will be analyzed in the following two theorems.

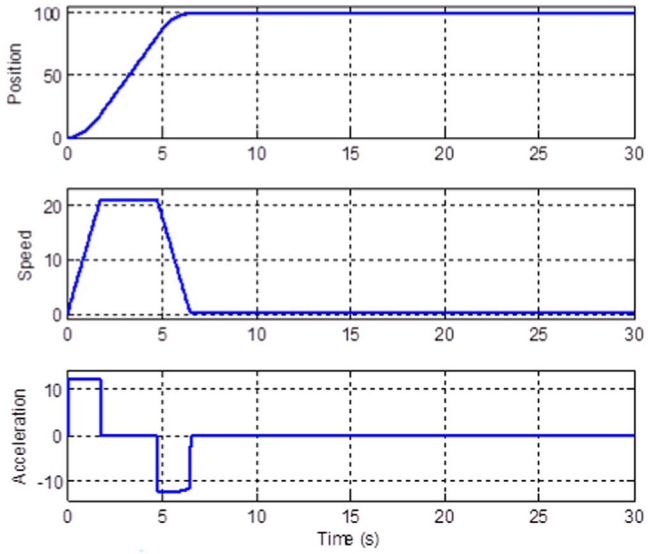

Figure 3. The outputs of the NLTD with speed upper bound.

3.1. The Convergence of VLTD

Theorem 1. *For VLTD, assume* $p_0(t) \equiv p_0$, $x_2(0) = 0$ *then for* $\forall x_1(0)$ *and* $\forall \sigma > 0$,$\exists t_c > 0$ *such that*

$$|x_1(t_c) - p_0| < 1 \tag{11}$$

***Proof**: Let* $z_1(t) = x_1(t) - p_0$, $z_2(t) = x_2(t)$, $\sigma_r = \sigma\sqrt{r}$, *then VLTD can be transformed to the following simplified form*

$$\begin{cases} \dot{z}_1(t) = z_2(t) \\ \dot{z}_2(t) = \begin{cases} -\sigma_r^2 r\,\mathrm{sgn}(z_1(t)) - 2\sigma_r z_2(t)/\sqrt{|z_1(t)|} & \text{if} |z_1(t)| \geqslant 1 \\ -\sigma_r^2 r z_1(t) - 2\sigma_r z_2(t) \quad if |z_1(t)| < 1 \end{cases} \end{cases} \tag{12}$$

Then we need to prove that, assume $z_2(0) = 0$, *for* $\forall x_1(t)$ *and* $\forall \sigma > 0$, $\exists t_c > 0$ *such that*

$$|z_1(t_c)| < 1.$$

Case1: if $|z_1(0)| < 1$, *then the variation law of the system conforms to the following equation*

$$\begin{cases} \dot{z}_1(t) = z_2(t) \\ \dot{z}_2(t) = -\sigma_r^2 z_1(t) - 2\sigma_r z_2(t) \end{cases} \tag{13}$$

The solution of the above differential equation is

$$z_1(t) = (z_1(0) + z_1(0)\sigma_r t + z_2(0)t)/e^{\sigma_r t} \tag{14}$$

As $z_2(0) = 0$, *then*

$$|z_1(t)| = |z_1(0)|(1 + \sigma_r t)/e^{\sigma_r t} < |z_1(0)| < 1. \tag{15}$$

The conclusion of the theorem holds.

Case2: if $z_1(0)| \geqslant 1$, *then the variation law of the system is*

$$\begin{cases} \dot{z}_1(t) = z_2(t) \\ \dot{z}_2(t) = -\sigma_r^2 - 2\sigma_r z_2(t)/\sqrt{z_1(t)} \end{cases} \tag{16}$$

From the second equation of (16), we can get

$$\dot{z}_2 = -\sigma_r^2 - \frac{2\sigma_r \dot{z}_1}{\sqrt{z_1}} = -\sigma_r^2 - (4\sigma_r\sqrt{z_1})' \tag{17}$$

Integral the above equation in the time interval $[0, \tau]$, *we can get*

$$\int_0^\tau \dot{z}_2(t)dt = \int_0^\tau -\sigma_r^2 - (4\sigma_r\sqrt{z_1})'\,dt \tag{18}$$

Then we can get

$$z_2(\tau) = -\sigma_r^2\tau - 4\sigma_r\sqrt{z_1(\tau)} + 4\sigma_r\sqrt{z_1(0)} \tag{19}$$

Integrate the above equation in the time interval $[0, t]$, *we can get*

$$z_1(t) = z_1(0) - \frac{\sigma_r^2 t^2}{2} + 4\sigma_r\sqrt{z_1(0)}\,t - 4\sigma_r\int_0^t \sqrt{z_1(\tau)}\,d\tau \tag{20}$$

If $\exists t_c \in [0, t]$, *s.t* $z_1(t_c) < 1$, *then the conclusion of the theorem holds. If* $z_1(\tau) \geqslant 1$ *for* $\forall \tau \in [0, t]$, *then*

$$\int_0^t \sqrt{z_1(\tau)}\,d\tau \geqslant t \tag{21}$$

that is

$$z_1(t) \leqslant -\sigma_r^2 t^2/2 + 4\sigma_r(\sqrt{z_1(0)} - 1)t + z_1(0) \tag{22}$$

Obviously, when $t > 4(\sqrt{z_1(0)} - 1)/\sigma_r$, *the right side of the above inequality is a monotonically decreasing function and*

$$\lim_{t \to +\infty} -\sigma_r^2 t^2/2 + 4\sigma_r(\sqrt{z_1(0)} - 1)t + z_1(0) = -\infty \tag{23}$$

Then there must exist $t_c > 0$, *such that*

$$-\sigma_r^2 t_c^2/2 + 4\sigma_r(\sqrt{z_1(0)} + z_2(0) - 4\sigma_r)t_c + z_1(0) < 1 \tag{24}$$

Thus

$$z_1(t_c) < 1. \tag{25}$$

The conclusion of the theorem holds.
Case3: if $z_1(0)| \leqslant -1$, *then the variation law of the system is*

$$\begin{cases} \dot{z}_1(t) = z_2(t) \\ \dot{z}_2(t) = \sigma_r^2 - 2\sigma_r z_2(t)/\sqrt{-z_1(t)} \end{cases} \tag{26}$$

From the second equation of (26), we can get

$$\dot{z}_2 = \sigma_r^2 - 2\sigma_r\dot{z}_1/\sqrt{-z_1} = \sigma_r^2 + (4\sigma_r\sqrt{-z_1})' \tag{27}$$

Integral the above equation in the time interval [0, τ] , we can get

$$\int_0^\tau \dot{z}_2(t)dt = \int_0^\tau \sigma_r^2 + (4\sigma_r\sqrt{-z_1})'\,dt \tag{28}$$

Then we can get

$$z_2(\tau) = \sigma_r^2\tau + 4\sigma_r\sqrt{-z_1(\tau)} - 4\sigma_r\sqrt{-z_1(0)} \tag{29}$$

Integrate the above equation in the time interval [0, t], we can get

$$\begin{aligned} z_1(t) = z_1(0) + \sigma_r^2 t^2/2 - 4\sigma_r\sqrt{-z_1(0)}\,t \\ + 4\sigma_r\int_0^t \sqrt{-z_1(\tau)}\,d\tau \end{aligned} \tag{30}$$

If $\exists t_c \in [0, t]$, s.t $z_1(t_c) > -1$, then the conclusion of the theorem holds. If $z_1(\tau) \leqslant -1$ for $\forall\tau \in [0, t]$, then

$$\int_0^t \sqrt{-z_1(\tau)}\,d\tau \geqslant t \tag{31}$$

that is

$$z_1(t) \geqslant \sigma_r^2 t^2/2 + 4\sigma_r(1 - \sqrt{-z_1(0)})t + z_1(0) \tag{32}$$

Obviously, when $t > 4(\sqrt{-z_1(0)} - 1)/\sigma_r$, the right side of the above inequality is a monotonically decreasing function and

$$\lim_{t \to +\infty} \sigma_r^2 t^2/2 + 4\sigma_r(1 - \sqrt{-z_1(0)})t + z_1(0) = +\infty \tag{33}$$

Then there must exist $t_c > 0$, s.t

$$\sigma_r^2 t^2/2 + 4\sigma_r(1 - \sqrt{-z_1(0)})t + z_1(0) > -1 \tag{34}$$

Thus

$$z_1(t_c) > -1. \tag{35}$$

The conclusion of the theorem holds.

Theorem 1 shows that, for the arbitrary initial value of x_1, there exists the time point t_c, which guarantees that VLTD can converge to the linear region.

Theorem 2. *Let t_c denote the time point when VLTD converges to the linear region, that is $|x_1(t_c) - p_0| < 1$, if $x_2(t_c)$ satisfies the following condition*

$$|x_2(t_c)| \leqslant (1 - |x_1(t_c) - p_0|)\sigma\sqrt{r} \tag{36}$$

then for $\forall\, t > t_c$, the following conclusion holds

$$|x_1(t) - p_0| < 1 \quad \text{and} \quad \lim_{t \to +\infty} x_1(t) = p_0.$$

***Proof**: According to Equation (12), we need to prove that if $|z_1(t_c) < 1|$ and $|z_2(t_c)| \leqslant (1 - |z_1(t_c)|)\sigma_r$, then for $\forall\, t > t_c$, we have*

$$|z_1(t)| < 1 \quad \text{and} \quad \lim_{t \to \infty} z_1(t) = 0.$$

Case1. If $t_c = 0$, that is $|z_1(0)| < 1$, since $z_2(0) = 0$, then according to (14), for $\forall\, t > 0$

$$\lim_{t \to +\infty} z_1(t) = \lim_{t \to +\infty} z_1(0)\frac{1 + \sigma_r t}{e^{\sigma_r t}} = 0. \tag{37}$$

The conclusion of the theorem holds.

Case2. If $|z_1(0)| \geqslant 1$, according to 1, there exists $t_c > 0$, such that $|z_1(t_c)| < 1$. Take t_c as the initial time point of the system, then the variation law of the system conforms to the following equation

$$\begin{cases} \dot{z}_1(t) = z_2(t) \\ \dot{z}_2(t) = -\sigma_r^2 z_1(t) - 2\sigma_r z_2(t) \end{cases} \quad t \geqslant t_c \tag{38}$$

Then we have

$$\begin{aligned} z_1(t) = (z_1(t_c) + z_1(t_c)\sigma_r(t - t_c) \\ + z_2(t_c)(t - t_c))/e^{\sigma_r(t - t_c)} \end{aligned} \tag{39}$$

Since $|z_2(t_c)| \leqslant (1 - |z_1(t_c)|)\sigma_r$, thus

$$\begin{aligned} |z_1(t)| &\leqslant (|z_1(t_c)||1 + \sigma_r(t - t_c)| + |z_2(t_c)|(t - t_c))/e^{\sigma_r(t - t_c)} \\ &\leqslant (|z_1(t_c)| + |z_1(t_c)|\sigma_r(t - t_c) \\ &\quad + (1 - |z_1(t_c)|)\sigma_r(t - t_c))/e^{\sigma_r(t - t_c)} \\ &< (1 + \sigma_r(t - t_c))/e^{\sigma_r(t - t_c)} \\ &< 1 \end{aligned} \tag{40}$$

That is for $\forall t > t_c$, the system is always in the linear region. Then

$$\lim_{t \to +\infty} |z_1(t)| \leqslant \lim_{t \to +\infty} (1 + \sigma_r(t - t_c))/e^{\sigma_r(t - t_c)} = 0. \tag{41}$$

The conclusion of the theorem holds.

Theorem 2 demonstrates that if VLTD enters the linear region at a speed satisfying some certain condition, then it will be always in the linear region until it converges to the set value.

3.2. The Speed and Acceleration Upper Bounds of VLTD

In this subsection, we will deduce the relationship between the speed and acceleration upper bounds of VLTD and its parameters. Let t_{vmax} denote the time point when VLTD reaches its maximum speed, then we have $\dot{x}_2(t_{\text{vmax}}) = 0$, that is

$$-r_1(t_{\text{vmax}})^2(x_1(t_{\text{vmax}}) - p_0) - 2r_1(t_{\text{vmax}})x_2(t_{\text{vmax}}) = 0 \tag{42}$$

we can get

$$|x_2(t_{\text{vmax}})| = r_1(t_{\text{vmax}})|x_1(t_{\text{vmax}}) - p_0|/2 \tag{43}$$

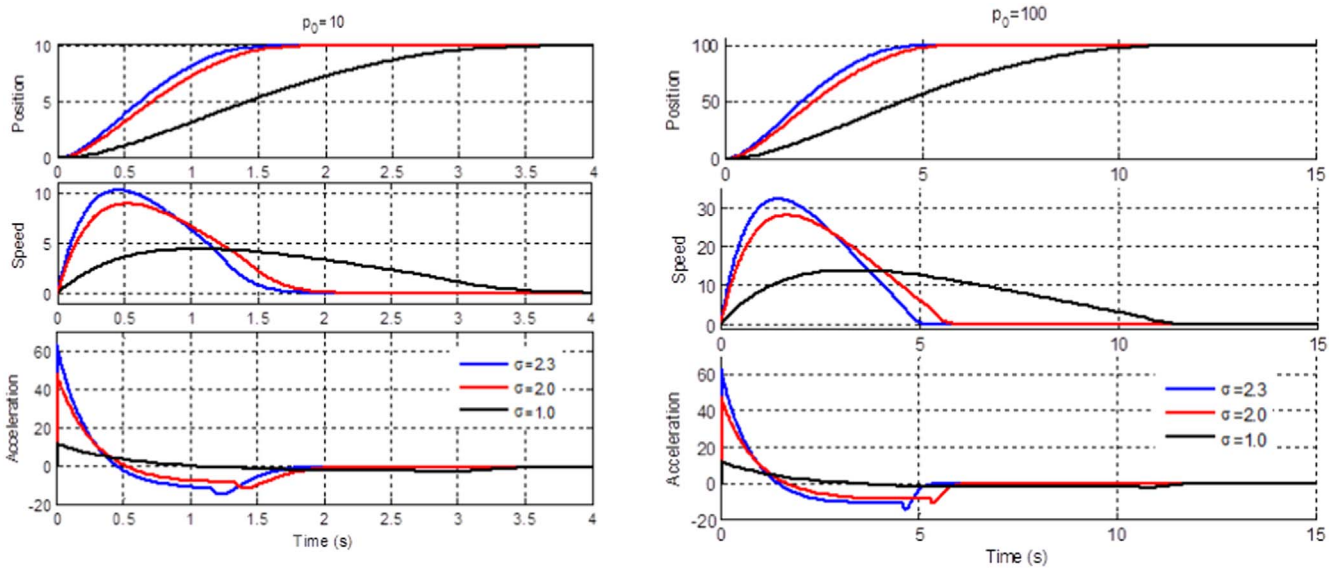

Figure 4. The outputs of VLTD, $p_0 = 10$(left), $p_0 = 100$(right).

if $|x_1(t_{\text{vmax}}) - p_0| < 1$, then

$$|x_2(t_{\text{vmax}})| < \sigma\sqrt{r}/2 \tag{44}$$

if $|x_1(t_{\text{vmax}}) - p_0| \geqslant 1$, then $r_1(t_{\text{vmax}}) = \sigma\sqrt{r}\Big/\sqrt{|x_1(t_{\text{vmax}}) - p_0|}$, that is

$$|x_2(t_{\text{vmax}})| = \sigma\sqrt{r|x_1(t_{\text{vmax}}) - p_0|}\Big/2 \tag{45}$$

According to the characteristic of VLTD, we have $|x_1(t_{\text{vmax}}) - p_0| \geqslant p_0/2$, so the maximum speed of VLTD satisfies the following condition

$$|x_2(t_{\text{vmax}})| \geqslant \sigma\sqrt{rp_0/8} \tag{46}$$

Equation (46) demonstrates that the speed output of VLTD will have no upper bound in the case when $x_1(t_{\text{vmax}}) - p_0 \geqslant 1$.

On the other hand, we can deduce that VLTD can reach its maximum acceleration at the initial time point and the acceleration upper bound is $\sigma^2 r$. Meanwhile, the acceleration of the acceleration section is significantly larger than the deceleration section. So in order to balance the speediness and the transitivity of VLTD, we should meticulously choose the parameter $\sigma > 1$ to guarantee that the acceleration in the deceleration section is not too small. Besides, in order to avoid a large acceleration impulse in the initial section, an acceleration upper bound will be added to the acceleration signal, which ensures the acceleration output of VLTD will not exceed the maximum acceleration of the physical system.

Therefore, it is necessary to add the speed and acceleration upper bounds to VLTD to ensure its transitional property. Let x_3 denote the acceleration signal contained in VLTD, $V_{\text{max\_VLTD}}$ denote the speed upper bound of VLTD, then the discrete form of VLTD with speed and acceleration upper bounds is described as follows

$$\begin{cases} x_2(k) = \text{sgn}(x_2(k))\min(|x_2(k)|,\ V_{\text{max\_VLTD}}) \\ x_1(k+1) = x_1(k) + hx_2(k) \\ x_3(k) = \begin{cases} -\text{sgn}(x_1(k) - p_0(k))\sigma^2 r - 2\sigma\sqrt{r}x_2(k)\Big/\sqrt{|x_1(k) - p_0(k)|} & if|x_1(k) - p_0(k)| \geqslant 1 \\ -\sigma^2 r(x_1(k) - p_0(k)) - 2\sigma\sqrt{r}x_2(k) & if|x_1(k) - p_0(k)| < 1 \end{cases} \\ x_3(k) = \text{sgn}(x_3(k))\min(|x_3(k)|,\ r) \\ x_2(k+1) = x_2(k) + hx_3(k) \end{cases} \tag{47}$$

It can be seen that it will not affect the convergence of VLTD when the speed and acceleration upper bounds are added.

4. Simulation Results

In this section, we show the simulation results of VLTD and give the comparison results of VLTD and NLTD. Assume that the maximum speed and acceleration of the physical system to be arranged are $V_{\text{max}} = 20$, $a_{\text{max}} = 12$. The sample period is $h = 0.001$ and three sets of parameters of VLTD are chosen as follows

$$\begin{aligned} \sigma_1 &= 1.0, \quad r = 12.0 \\ \sigma_2 &= 2.0, \quad r = 12.0 \\ \sigma_3 &= 2.3, \quad r = 12.0 \end{aligned} \tag{48}$$

For analysis, the set values are chosen as $p_0 = 10$ and $p_0 = 100$, respectively. Figure 4 demonstrates the output signals of VLTD for the different cases. It can be seen that the maximum speed will increase as the parameter σ or p_0 increases, which is consistent with Equation (46). The maximum acceleration will increase as parameter σ increases, but it has no relationship with p_0.

Figure 5 gives the comparison plots of VLTD with and without upper bounds in the case $\sigma = 2.3$ and $p_0 = 100$. The

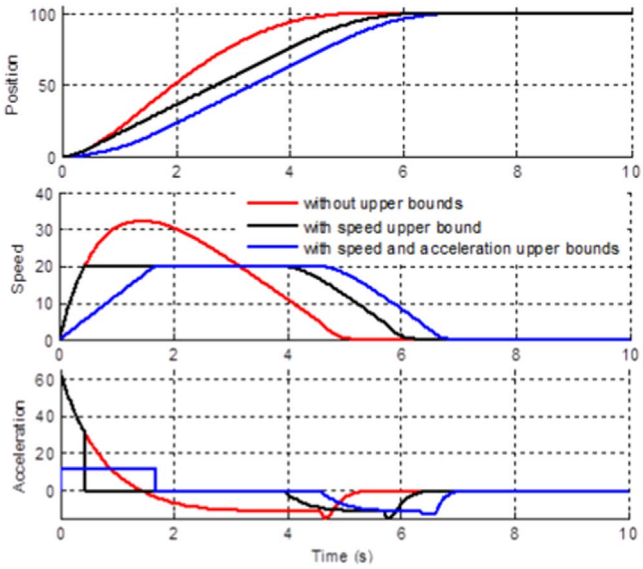

Figure 5. Comparison plots of the VLTD with and without speed and acceleration upper bounds.

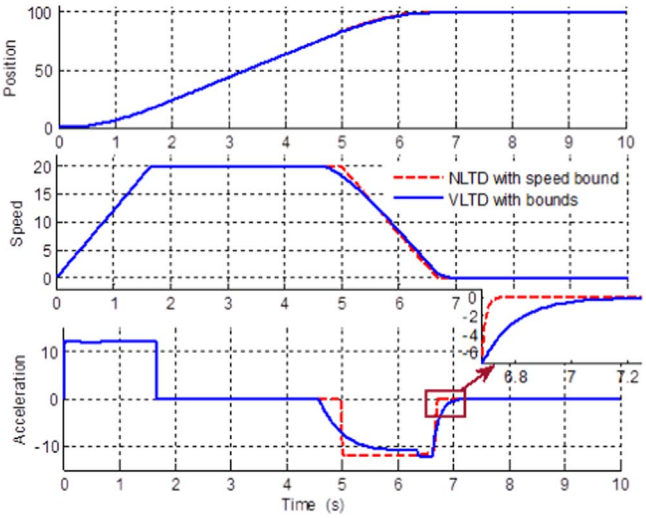

Figure 6. Comparison plots of VLTD and NLTD.

speed and acceleration upper bounds are chosen as $V_{\max \mathrm{VLTD}} = 20$ and $r = 12$, respectively.

It demonstrates that VLTD with speed and acceleration upper bounds can converge to the set value with a certain speed and acceleration, which is consistent with the feedback capability of the physical system.

Next, VLTD with speed and acceleration upper bounds will be called the VLTD with bounds in abbreviation. Clearly, the implementation of the VLTD with bounds is distinctly easier than NLTD mentioned in Section 2.2. Figure 6 gives the comparison plots of the VLTD with bounds and NLTD with

Figure 7. 1 meter aperture ground-based telescope and the driver hardware.

speed upper bounds. It shows that the VLTD with bounds can achieve almost the same results as NLTD in the acceleration section and from the third subplot we can see that the acceleration signal contained in the VLTD with bounds is smoother than NLTD in the deceleration section, which is favorable in the transition process arrangement.

5. Experiment Results on Some 1 Meter Ground-based Telescope

In this section, we will apply the VLTD with bounds to the main axis control of the 1 m aperture ground-based telescope shown in Figure 7. As the telescope is used for the astronomical observations, the observational efficiency is a very important index for the telescope. So it is important to give a reasonable transitional signal for the position reference signal to guarantee both efficiency and stability of the system. The main axis of the telescope is driven by a permanent magnet synchronous motor (PMSM), and the hardware platform is realized based on the DSP-TMS320F28335 and FPGA-EP3C40F324. The position sensor is a 29 bits absolute

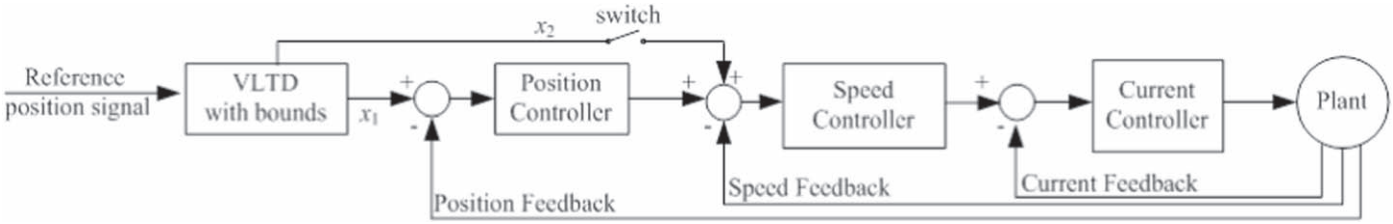

Figure 8. The total block of the system.

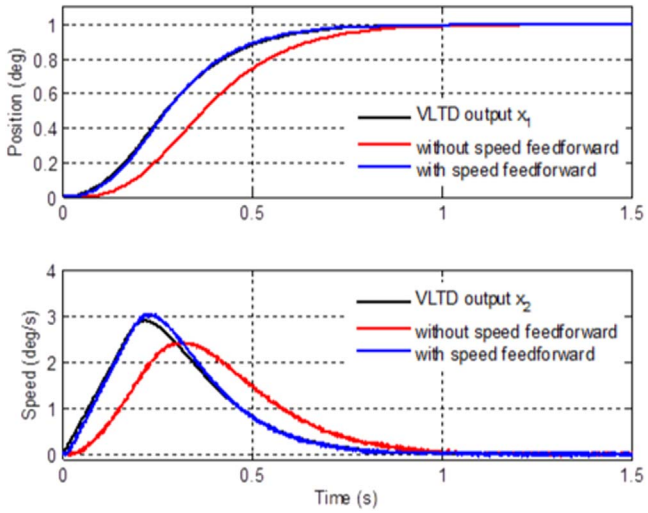

Figure 9. The position step response of VLTD when $p_0 = 1$.

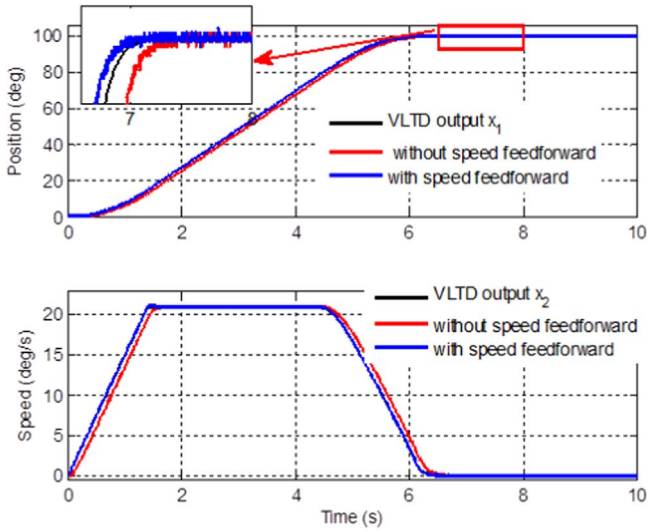

Figure 11. The position step response of VLTD when $p_0 = 100$.

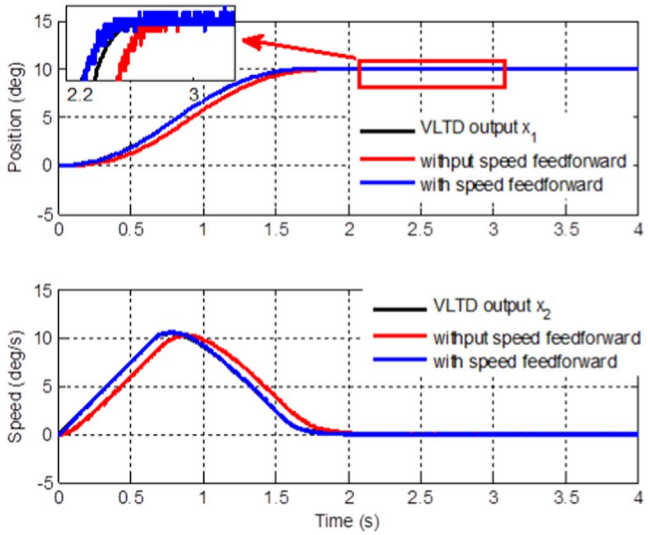

Figure 10. The position step response of VLTD when $p_0 = 10$.

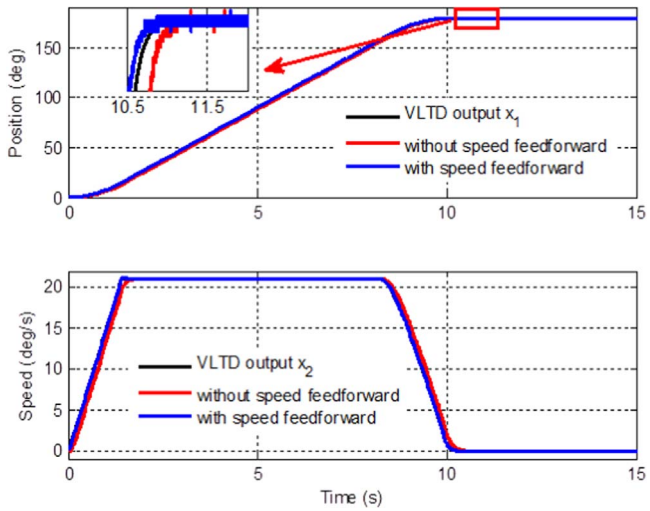

Figure 12. The position step response of VLTD when $p_0 = 180$.

Table 2
The Time Points for the Position Response to Enter 5″ and 1″ Error Bands by Using VLTD

	Set values	Without speed feed forward	With speed feed forward
1	Time point(5″ error band)	1.233 s	1.047 s
	Time point(1″ error band)	1.429 s	1.243 s
10	Time point(5″ error band)	2.258 s	2.025 s
	Time point(1″ error band)	2.436 s	2.181 s
100	Time point(5″ error band)	6.802 s	6.567 s
	Time point(1″ error band)	6.979 s	6.772 s
180	Time point(5″ error band)	10.612 s	10.381 s
	Time point(1″ error band)	10.791 s	10.532 s

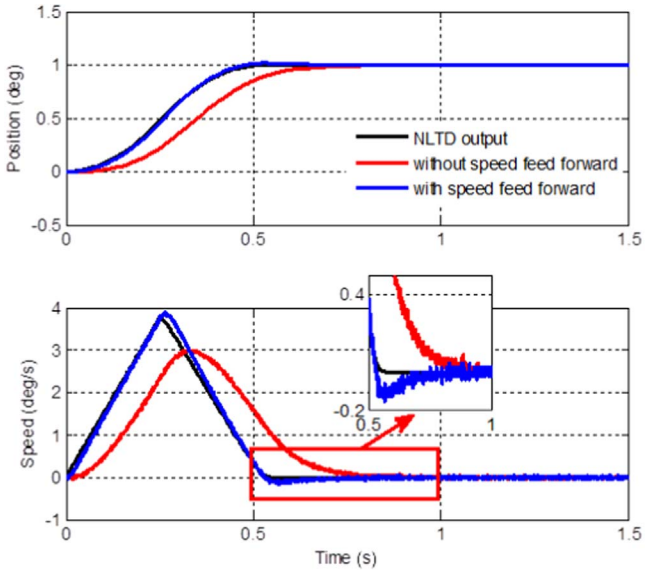

Figure 13. The position step response of NLTD when $p_0 = 1$.

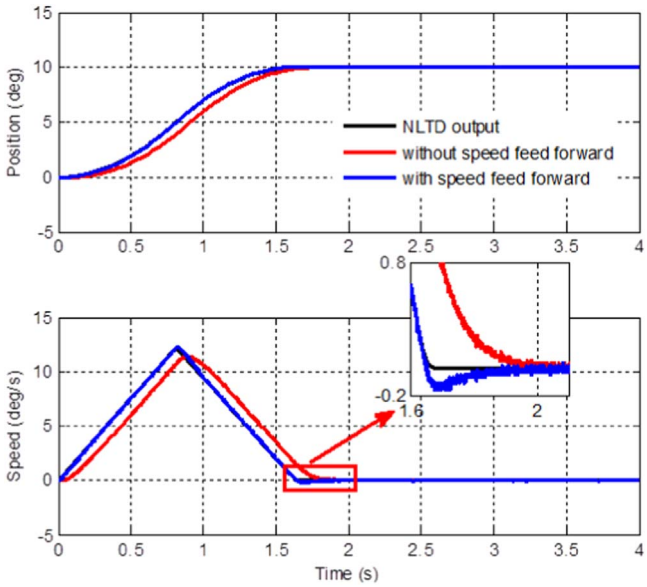

Figure 14. The position step response of NLTD when $p_0 = 10$.

encoder, and the speed feedback information is obtained by the differential of the encoder. The transition process arrangement and the control algorithm are both realized on the DSP platform.

Actually, the maximum speed and acceleration of the azimuth axis are determined by not only the maximum output power of the driving power supply but also the motor and mechanical parameters. The parameters related are as follows

$$\begin{aligned} &U_{dc} = 48\text{V}, I_{dc} = 10\text{A}, \\ &K_m = 12880\text{V}(1000\text{rpm})^{-1}, \\ &K_e = 116.3\text{NmA}^{-1}, J = 4000\text{kg} \cdot \text{m}^2 \end{aligned} \tag{49}$$

where U_{dc} and I_{dc} denote the bus-bar voltage and current of the power supply, K_m and K_e are the EMF coefficient and torque constant of the motor, J is the azimuth inertia of the axis.

After calculation, the maximum angular speed and acceleration of the azimuth axis are $22.4\text{deg} \cdot \text{s}^{-1}$ and $16.7\text{deg} \cdot \text{s}^{-2}$, respectively. In order to maximize the tracking efficiency of the system, the maximum speed and acceleration are both slightly smaller than the maximum output of the physical system, which will facilitate the stability of the control system.

$$V_{\max\_\text{VLTD}} = 21,\ r = 15,\ \sigma = 2.3 \tag{50}$$

The total block of the system is shown in Figure 8 where the speed output x_2 of VLTD can be treated as the speed feed forward information to the speed controller. The current controller was designed as the classical PI controller, and the speed controller was designed as the PI controller with the 2nd order ESO compensation (Yang et al. 2021). As the inner control loop has a good capability of disturbance rejection, the position controller would be designed as the simplest proportional controller which can be easily implemented. Parameters for the three-loop controllers and the 2nd order

Table 3
The Time Points for the Position Response to Enter 5″ and 1″ Error Bands by Using NLTD

Set values		Without speed feed forward	With speed feed forward
1	Time point(5″ error band)	0.896 s	0.728 s
	Time point(1″ error band)	1.027 s	0.893 s
10	Time point(5″ error band)	2.022 s	1.887 s
	Time point(1″ error band)	2.157 s	2.021 s
100	Time point(5″ error band)	6.553 s	6.425 s
	Time point(1″ error band)	6.680 s	6.551 s
180	Time point(5″ error band)	10.360 s	10.232 s
	Time point(1″ error band)	10.550 s	10.361 s

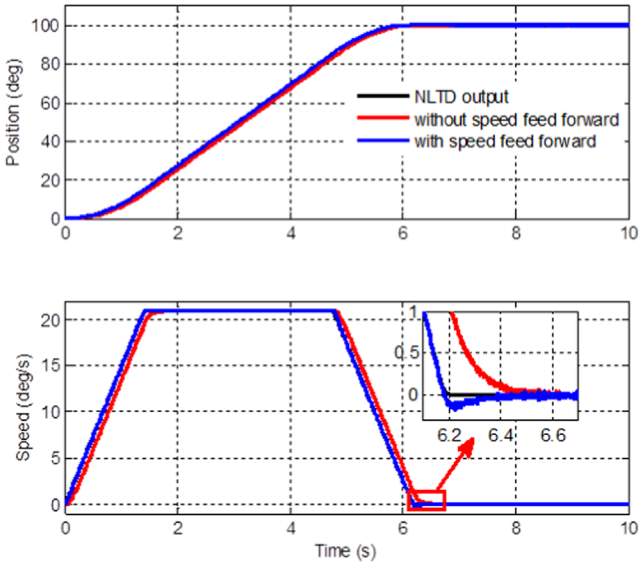

Figure 15. The position step response of NLTD when $p_0 = 100$.

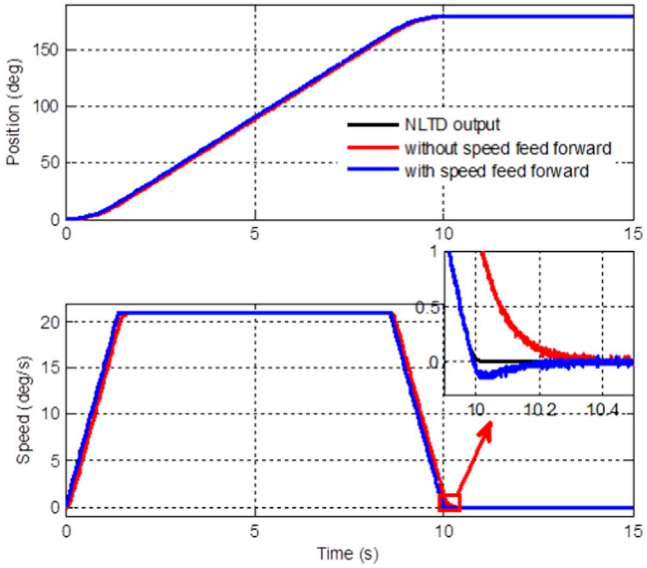

Figure 16. The position step response of NLTD when $p_0 = 180$.

ESO are listed as follows

$$b = 0.05,\ \omega_0 = 40,\ I_{Kp} = 10,\ I_{Ki} = 0.2,$$
$$V_{Kp} = 70,\ V_{Ki} = 0.01,\ P_{Kp} = 0.01 \quad (51)$$

where b denotes the ESO parameter, ω_0 denotes the bandwidth of ESO, I_{Kp} and I_{Ki} denote the proportional and integral coefficients of the current controller, V_{Kp} and V_{Ki} denote the proportional and integral coefficients of the speed controller, and P_{Kp} denotes the proportional coefficient of the position controller.

To give a comparison, experiments with and without speed feed forward are both conducted on the 1 m telescope using the same controller. Since the azimuth axis of the telescope has no mechanical limit, the maximum step size of the azimuth axis is 180deg according to the principle of proximity. Figures 9–12 give the experimental results of the position step response when $p_0 = 1$, 10, 100, 180. As the acceleration feedback signal was obtained by twice-differential of the encoder measurement which was seriously polluted by the measurement noise of the 29 bits encoder, Figures 9–12 only demonstrate the position and speed response plots of the system.

It can be seen that the control method with speed feed forward can speed up the reaction of the system distinctly. From the zoom in figures we can see that the position responses can reach the set values fast and without overshoot by using VLTD to arrange the transition process. Table 2 gives the time points at which the tracking errors enter 5″ and 1″ error band for each experiment. It describes the effect of the speed feed forward quantitatively.

For further comparison, we have done the experiments using the NLTD with speed upper bound to arrange the transition process. That is replacing VLTD block in the Figure 8 with NLTD block. Similarly, the experiments with and without speed feed forward were both done for the NLTD case where

the parameters were chosen as follows

$$V_{\max\_\mathrm{NLTD}} = 21,\ r = 15 \tag{52}$$

Figures 13–16 give the comparison results of the experiments using the NLTD with and without speed feed forward. It shows that although the speed feed forward information can speed up the reaction of the system, it brings distinct over shoot phenomenon for the position and speed response. Table 3 gives the time points at which the tracking errors enter 5″ and 1″ error band for each experiment using NLTD. Comparing the fourth column of Table 2 and the third column of Table 3, we can see that the VLTD with speed feed forward can obtain almost the same results with the NLTD without speed feed forward. Meanwhile, the calculation time of VLTD is almost $1/6$ as that of NLTD, which is favorable for the timely implementation of the algorithm in engineering practice.

6. Conclusion

In this paper, a VLTD with speed and acceleration upper bounds, which is used to arrange the transition process for the physical systems, has been proposed. It can not only play a transitional role in the transition process arrangement, but also can maximize the tracking ability of the system. The analyzed convergence result of VLTD demonstrates that for the arbitrary initial value of VLTD, it can converge to the linear region in a limited time and it will be always in the linear region until it converges to the set value when its speed satisfies some certain condition.

The simulation results show that VLTD, which has a smooth speed and acceleration with upper bounds, can achieve a practical transition process for the physical system. It is convenient to implement, because it has only one adjustable parameter to be tuned once the speed and acceleration upper bounds are determined. The experiments on some 1 meter ground based telescope give the comparison results of VLTD and NLTD, which showed that VLTD can get almost the same performance as NLTD while the implementation of VLTD is much simpler than NLTD.

Although all of the above analyses are based on the constant set values, VLTD can also be applied to tracking the time-varying signals. The properties for tracking time-varying signals will be conducted in the follow-up studies.

Acknowledgments

This work was supported in part by the National Natural Science Foundation of China under Nos. 12122304 and 11973041, and in part by the Youth Innovation Promotion Association CAS, under No. 2019218.

References

Bu, X. W., Wu, X. Y., Chen, Y., & Bai, R. 2015, Int. J. Control Auto. Syst., 13, 595
Guo, B., & Zhao, z. 2013, ITAC, 58, 1074
Han, J. 1989, J. Sys. Sci. Math. Sci., 9, 328
Han, J. 2009, ITIE, 56, 900
Han, J., & Wang, W. 1994, J. Sys. Sci. Math. Sci., 14, 177
Han, J., & Yuan, L. 1999, J. Sys. Sci. Math. Sci., 19, 268
Qi, G., Chen, Z., & Yuan, Z. 2004, J. Syst. Eng. Electron, 15, 780
Tang, Y. G., Wu, Y. W. M. H. X., & Tang, Y. G. 2009, IEEE J. Sel. Top. Signal. Proc, 3, 716
Tian, D. P., Shen, H., & Dai, M. 2014, ITIE, 61, 3736
Wu, L. Q., Lin, H., & Han, J. 2004, J. Syst. Simu., 16, 651
Xie, Y. D., Zhang, H. S. L. G. Z. C. & TSO 2019, IEEE Access, 7, 101941
Yang, X. X., Deng, Y. T., Zhang, B., & Wang, J. L. 2021, RAA, 21, 316
Yang, Z. B., Ji, J. S. X. Z. H., & Zhao, Q. 2020, IEEE J. Emerg. Sel. Top. Power Electron., 8, 2623
Yu, j., & Jin, s. 2021, IEEE Access, 6, 86017
Zhang, h., Xiao, G., & Yu, X. 2021, ITIE, 68, 3359
Zhang, H., Xie, Y. X. G. Z. C., & Long, Z. 2019, IEEE Trans. Cont. Tech., 27, 1728
Zhao, L., Yang, Y. X. Y., & Liu, Z. 2015, ITIE, 62, 5838